Zootaxa 5397 (3): 377–396
https://www.mapress.com/zt/

Article

ISSN 1175-5326 (print edition)
ZOOTAXA
ISSN 1175-5334 (online edition)

https://doi.org/10.11646/zootaxa.5397.3.4
http://zoobank.org/urn:lsid:zoobank.org:pub:35CF5F2E-5710-4C08-8734-0540EC521674

Three new interstitial species of the genus *Neonesidea* (Bairdioidea: Podocopida: Ostracoda) from the infralittoral zone in Japan

ERIKA ASABA[1,2], REINA ASABA[1,3] & AKIRA TSUKAGOSHI[1,4*]
[1]*Graduate School of Integrated Science and Technology, Shizuoka University, 836 Ohya, Suruga-ku, Shizuoka City, 422–8529 Japan*
[2] *asaba.erika.16@shizuoka.ac.jp;*
[3] *asaba.reina.18@shizuoka.ac.jp;*
[4] *tsukagoshi.akira@shizuoka.ac.jp; https://orcid.org/0000-0002-1402-9627*
**Corresponding author*

Abstract

This study is the first to report on interstitial species of the genus *Neonesidea*: *Neonesidea arenalocus* **sp. nov.** from the Pacific coast of central Japan, *Neonesidea alyamanai* **sp. nov.** from the Pacific coast of south-western Japan, and *Neonesidea alwakasaensis* **sp. nov.** from the Sea of Japan coast of western Japan. All three species share a smaller carapace size than that of the epiphytic *Neonesidea* species; in particular, the carapace width and valve thickness are significantly less. Furthermore, the terminal claws on the walking legs are more linear than those of the epiphytic *Neonesidea* species. However, these three new species share a feature in the apical portion of the terminal claw on the male's second antennae and asymmetric brush-shaped organs, which are common to this genus. In addition, the results of our field survey indicate that all three new species occur in coarse-grained sediments (coarse sand to pebbles) in the upper infralittoral zone, particularly on Miho-Masaki Beach, which contains an optimum zone for *N. arenalocus* **sp. nov.**

Key words: Arthropoda, X-ray micro CT scan, optimum zone, brush-shaped organ, grain-size composition

Introduction

The phylogenetic origin of bairdiid ostracods can be traced back to the Early Palaeozoic (Howe 1955; van Morkhoven 1963). The modern systematic concept of the family Bairdiidae was proposed by Maddocks (1969), and it has been widely accepted by ostracod researchers. The Recent superfamily Bairdioidea is considered to include the three families Bairdiidae, Bythocyprididae, and Pussellidae (Horne *et al.* 2002); among these, only the Pussellidae comprises entirely interstitial taxa. The bairdiid genus *Noenesidea* is widely distributed in shallow waters at low and mid-latitudes, with more than 80 species known to date (Brandão 2020); however, *Neonesidea* species from interstitial environments have not been reported thus far.

Cerca *et al.* (2018) provided a comprehensive solution for the geographical distribution and taxonomic diversity of interstitial meiofauna. Previously, it was reported that interstitial species exhibit universal distribution contrary to their sedentary life style (the 'meiofauna paradox'); however, Cerca *et al.* (op. cit.) noted that this is a problem due to taxonomic resolution stemming from morphological similarity and that the geographical distribution of interstitial species is narrow. We fully agree with this view. Indeed, the interstitial ostracods described so far around Japan also have a narrow geographical distribution range and are divided into many independent species. (Tanaka *et al.* 2010; Higashi & Tsukagoshi 2011; Higashi *et al*. 2011; Tanaka & Tsukagoshi 2013b, 2014; Tanaka *et al.* 2014; Ito & Tsukagoshi 2022, and so on). The ostracods, especially the Podocopa, have well-developed male copulatory organs, and their morphology makes the species classification clear. This is in contrast to the convergence of the carapace and appendages becoming smaller and simpler in order to adapt to the interstitial environment (Tsukagoshi 2017). Therefore, actual "species identification" can be easily performed based on the morphology. Tsukagoshi (2017) suggests that interstitial species of ostracods have large species diversity comparable to epiphytic species. It is likely that the undescribed species of the interstitial genus *Neonesidea* are not limited to those reported here, and that many other species exist as undescribed or cryptic species.

Accepted by R. Smith: 12 Oct. 2023; published: 5 Jan. 2024

Most of the reports on interstitial ostracods from Japan are concentrated in the intertidal zone (Higashi & Tsukagoshi 2008, 2011, 2012; Higashi *et al*. 2011; Hiruta 1983, 1989, 1991; Tanaka 2013; Tanaka & Ohtsuka 2016; Tanaka & Tsukagoshi 2013a, 2013b, 2014; Tanaka *et. al*. 2010, 2014; Ha & Tsukagoshi 2015; Watanabe *et al*. 2008; Yamada & Tanaka 2011, 2013). Other studies have reported their presence in the supralittoral zone (Hiruta *et al.* 2007) and in estuaries, which are a part of the intertidal zone (Tanaka & Tsukagoshi 2010; Tanaka *et al*. 2014). Additionally, they can be found at a depth of more than 10 m from the sea floor (Tanaka & Ohtsuka 2019; Tanaka *et al.* 2020). However, since these species were collected from relatively deep water using samplers, it is unclear whether they are strictly interstitial species.

In contrast, there are only two reports on ostracods from the infralittoral zone around the strand line in Japan (Yamada & Tanaka 2013; Ito & Tsukagoshi 2022). They collected the species from around or just under the strand line during the lowest spring tide. The present study attempted sediment collection from a slightly deeper depth of around 0.5 m than what has been previously reported.

Compared to the intertidal zone, collecting samples of interstitial species from the infralittoral zone, where the water depth is approximately 0.5 m, is more difficult. However, this depth permits precise observations at fixed points. Watanabe *et al.* (2008) showed the different optimum zones for different species of interstitial ostracods and the relationship between sediment grain size composition and population density in the intertidal zone. In the same way, in the present study, we explored the optimum zone and preferred grain-size composition for *Neonesidea arenalocus* **sp. nov.** in the upper infralittoral zone. Additionally, we detected the interstitial ostracod fauna of the upper infralittoral zone at a water depth of approximately 0.5 m for the first time, suggesting that a unique ostracod fauna is present in the infralittoral zone, which is different from that in the intertidal zone.

The descriptions of three new species in this study provide new information on the diversity of interstitial species, an aspect that has hitherto been poorly described. At the same time, this detailed study of the optimum zone and the characteristics of the co-occurring species will provide new insights into the adaptation of ostracods to interstitial environments and their evolution.

Materials and methods

Specimens of three new interstitial *Neonesidea* species were collected from coarse sand to pebble beach sediments (sediment depth: approximately 0.5 m) under the strand line during the lowest spring tide at Miho-Masaki Beach, Shizuoka City, Shizuoka Prefecture (35° 01′ 14″ N, 138° 31′ 15″ E; Loc. 1 in Fig. 1 and Fig. 2A), on 18 June 2015; Motojima, Tanabe City, Wakayama Prefecture (33° 43′ 56″ N, 135° 20′ 58″ E; Loc. 2 in Fig. 1) on 19 September 2015; and Tai Beach, Miyazu City, Kyoto Prefecture (35° 34′ 53″ N, 135° 14′ 10″ E; Loc. 3 in Fig. 1) on 9 September 2016. Sampling at fixed points was performed at Loc. 1 (Fig. 1 and Fig. 2A), and sediment materials were collected at points separated by a distance of 0.5 m along a fixed transect from the strand line 18 m away from a landmark to 3.5 m offshore (Fig. 2B). Each sample consisted of a scoop of 500 ml of sediments, collected after digging five times to remove surface sediments in the seawater (Fig. 2B). The three epiphytic *Neonesidea* species for our comparison were collected from seaweeds in the intertidal zone of Omotehama, Miura City, Kanagawa Prefecture (35° 09′ 36″ N, 139° 36′ 42″ E) on 26 March 1982 and on 6 December 2017.

Each sample was washed five times in a bucket, and the top layer of water was strained through a 50 μm mesh net. Ostracod specimens were retrieved from the residue remaining in the net using a binocular microscope, and their individual numbers were counted (Fig. 2C). For permanent storage, most of the collected samples were fixed in approximately 5 % formaldehyde solution neutralised with hexamethylenetetramine, and then transferred to 70–80% alcohol solution. The soft parts were dissected and mounted in Neo-Shigaral medium on glass slides, observed under a light transmission microscope (BX-50, Olympus Life Science) with a camera lucida attached, and sketched. The sketches were digitised using a printer coupled with a scanner (EP-882AW, Epson). Carapaces were observed using a scanning electron microscope (JSM-5600LV, JEOL) after freeze-drying (Aqua FD-6500, Sun Technologies) and coating with osmium ion (OPC40, Filgen). For measurements, an optical stereo-microscope with an ocular micrometre or a digital micrometre (digital linear gauge D-10S, Peacock Ozaki Mfg) was used. The transverse sections of the carapace of epiphytic and interstitial *Neonesidea* species were observed using X-ray micro-computed tomography (CT) scans (Scan X mate-E090, Comscantecno).

At each sampling point of Loc. 1 (Fig. 2B 1–8, 100 ml sediment was collected separately to analyse the grain-

size composition of the sediment. Each sediment was lightly washed in fresh water and dried, and then the sediments were sieved through five meshes with openings of 8 mm, 4 mm, 2 mm, 1 mm, and 0.5 mm. Grains larger than 8 mm in size were removed in advance, and the weight (%) of grains of sizes 8–4 mm, 4–2 mm, 2–1 mm, 1–0.5 mm, and <0.5 mm was measured to derive the grain-size composition (Fig. 3).

To characterise the interstitial species, the curvature of the terminal claws of the fifth, sixth, and seventh limbs of three interstitial species and three epiphytic species were compared. The straight-line distance from the proximal end to the tip of the terminal claw (A) and the perpendicular distance from the straight line to the apex of the maximum curvature (B) were measured, and B/A denoted the curvature (Fig. 4). The software ImageJ (ver. 1.51) was used for the measurements.

All illustrated specimens have been deposited in the collection of the Shizuoka University Museum with the prefix SUM-CO.

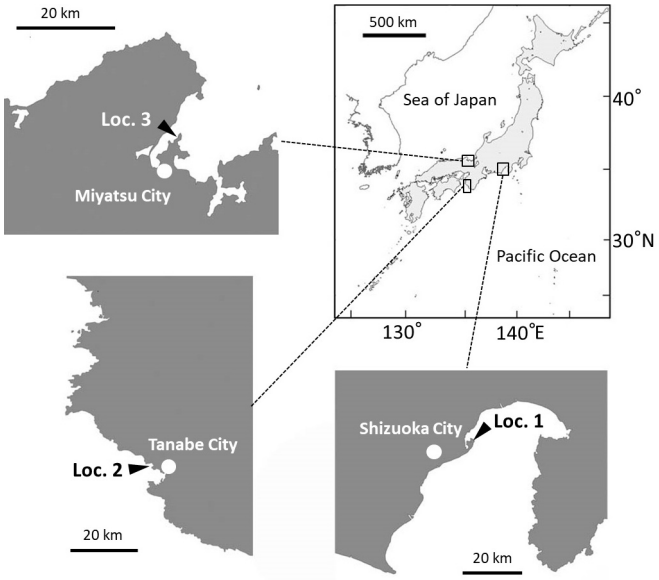

FIGURE 1. Map showing the sampling localities of *Neonesidea* species. Miho-Masaki Beach (Loc. 1), Motojima (Loc. 2), and Tai Beach (Loc. 3).

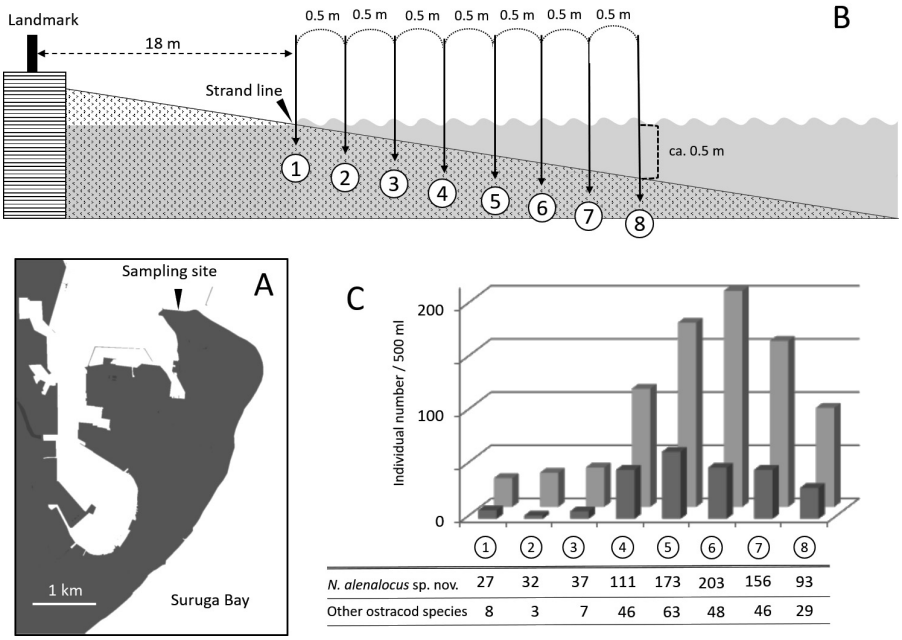

FIGURE 2. Sampling in Miho-Masaki Beach (Loc. 1 in Fig. 1). A, detailed location of Miho-Masaki Beach (Loc. 1). B, sampling scheme in Loc. 1, sediment materials were collected at eight points at 0.5 m intervals. C, individual number / 500 ml of *Neonesidea arenalocus* **sp. nov.** (grey bars at the back) and other ostracod species (black bars at the foreground). Materials were collected on 18 June 2015.

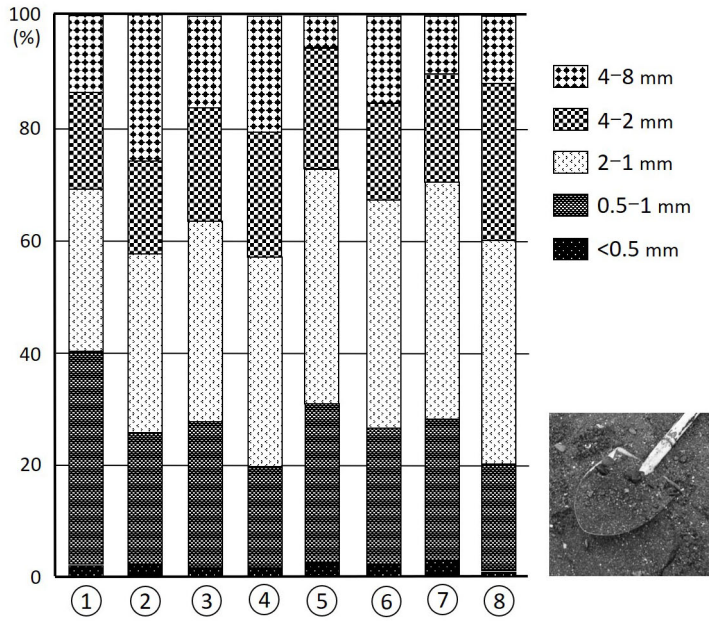

FIGURE 3. Grain size composition of the sediment at eight points in Miho-Masaki Beach (Loc. 1 in Fig. 1 and Fig. 2). The numbers correspond to Fig. 2B and C. Materials were collected on 18 June 2015.

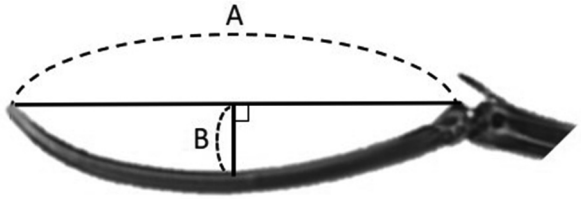

FIGURE 4. Method for measuring the curvature of the terminal claws of the fifth, sixth, and seventh limbs of the three interstitial and the three epiphytic species. The straight-line distance from the proximal end to the tip of the terminal claw (A) and the maximum perpendicular distance from the straight line to the apex (B) were measured, and B/A was used as the curvature.

Results

Population density of *Neonesidea arenalocus* sp. nov. along the fixed transect and grain-size composition in Miho-Masaki Beach and the co-occurring ostracod species

Population density (number of individuals /500 ml sediment) of *Neonesidea arenalocus* **sp. nov.** along the fixed transect in Miho-Masaki Beach (the type locality) is shown in Fig. 2C. The density was more than 100 individuals at each point between 1.5 m and 3 m from the strand line at the lowest spring tide, with the maximum density (203 individuals) at 2.5 m. The main ostracod species that co-occurred include *Parvocythere japonica* Watanabe *et al.,* 2008, *Parapolycope* spp., *Cytherois* sp., *Parvocythere* spp., *Cobanocythere* sp., *Tribelina* sp., *Semicytherura sagittiformis* Yamada & Tanaka, 2011, and so on. We did not find any significant difference in the grain-size composition of the collected sediments from the points (Fig. 3). At all points, 1–2 mm grain-size sand was predominant.

Comparison of the curvature of the terminal claws on the fifth to seventh legs between interstitial and epiphytic *Neonesidea* species

The curvature of the terminal claws on the fifth, sixth, and seventh limbs of the three interstitial species and three epiphytic species of *Neonesidea* are shown in Table 4. The curvatures in the interstitial species are lower (near-straight) on the sixth and seventh limbs compared to the fifth limb. In the epiphytic species, the same tendency was

found in *Neonesidea* sp. 1 and *N*. sp. 2, but not in *N*. sp. 3. The average values of the three limbs between the three interstitial (0.18 and lower) and three epiphytic species (0.21 and higher) were clear. Overall, the interstitial species had straighter terminal claws than the epiphytic species.

Taxonomy

Superfamily Bairdioidea Sars, 1888

Family Bairdiidae Sars, 1888

Genus *Neonesidea* Maddocks, 1969

Neonesidea arenalocus sp. nov.

(Figs. 5, 6, 7A, B, 12C, D)

Neonesidea sp. I: Ito & Tsukagoshi 2022, Fig. 8 and Tables 1–3.

Type series. All examined specimens collected at the upper infralittoral zone of coarse sand beach in Miho-Masaki Beach, Shizuoka City, Shizuoka Prefecture (35° 01′ 14″ N, 138° 31′ 15″ E; Loc. 1 in Fig. 1) on 18 June 2015. Holotype: adult male (SUM-CO-2522), right valve length 0.89 mm, height 0.44 mm, left valve length 0.88 mm, height 0.48 mm, appendages mounted on glass slide and valves preserved in cardboard cell slide. Paratypes: 5 adult males (SUM-CO-2517, 2518, 2521, 2523 and 2524) and 3 adult females (SUM-CO-2519, 2520 and 2525).

Etymology. Latin *arena* (sand) and *locus* (space), owing to the habitat of this species.

Description. *Carapace* (Figs. 5 and 12C, D) small and thin, compressed laterally, streamlined subhexagonal in lateral view. Dorsal margin of right valve almost straight, making slightly steep slope with ventral margin. Biconvex-lens shape in dorsal view. Carapace epidermis semi-translucent. Surface throughout smooth with numerous sensilla of simple-type pore systems. Left valve larger and rounder than right valve, and overlapping right valve along dorsal and ventral margins. Anterior and posterior margins of right valve developing frills, posterior one serrated. Left valve without frill. Adductor muscle scars consisting of 8 elongated diagonally. Mandibular scar separated in two. Fulcral point just in front of top row of adductor muscle scars. Hingement weak and simple: right valve bearing simple bar with dorsal groove; left valve bearing groove with dorsal shelf. More than 10 auxiliary fine dentitions at centre of interior ventral margin in male left valve, but no complementary structure in right valve.

Eye. Naupliar eye. No eye spot on carapace.

Antennula (Fig. 6A). Seven articulated podomeres, approximate length ratio among them from proximal to distal 15: 8: 2: 3: 1: 2: 2. Three terminal podomeres with much longer setae than total length of antennule podomeres. First podomere with a few comb-like rows of setulae at antero-distal corner. Second podomere with 1 medium seta on posterior margin. Third podomere with 1 long apical seta on posterior distal end and 2 very short setae at antero-distal corner. Fourth podomere with 1 short apical seta at both anterior and posterior corners, respectively. Fifth podomere with 2 very long setae on both antero- and postero-distal ends. Sixth podomere with 2 and 3 very long setae on antero- and postero-distal ends, respectively. Seventh (terminal) podomere with 5 very long setae on distal end.

Antenna (Fig. 6Bm). Male with 5 articulated podomeres, approximate length ratio among them from proximal to distal 13: 9: 5: 18: 3. First podomere (protopodite) bearing 1 long and 1 medium-length setae on distal margin and assemblage (reduced exopodite) of 1 long and 2 short setae in distal end. Second podomere bearing 3 long setae on postero-proximal margin, and 1 long and 1 medium-length apical seta at postero-distal corner. Third podomere with 1 long and 1 medium-length setae at postero-distal corner. Fourth podomere with 1 short seta on middle of anterior margin, 1 medium-length setulous apical seta at postero-distal corner and 2 short apical setae on antero-distal margin, and assemblage of numerous short setulae along postero-distal margin. Fifth (terminal) podomere of male bearing 1 large terminally bifurcated claw with 1 tiny spine on posterior-distal margin, 1 short seta on antero-distal margin and 1 medium setulous seta on posterior-distal margin. Female antenna similar to that of male except fifth podomere (Fig. 6Bf) bearing 2 terminal claws, and 1 long and 1 medium-length seta on distal end.

Mandible (Fig. 6C) consisting of 5 podomeres, approximate length ratio among them from proximal to distal

30: 7: 4: 6: 4. First podomere (coxa) bearing masticatory part of 4 stout denticles, several very short thin setae on distal end, and one short simple seta on anterior margin. First podomere of palp (basis) with 1 medium-length seta and 1 short seta on antero-distal corner and middle of distal end, respectively. Branchial plate (reduced exopodite) consisting of 1 very long stout setulous, 1 long and 1 medium-long setulous setae on dorso-proximal margin. Second podomere of palp (1st podomere of endopodite) with 2 setae on anterior-distal end, 1 seta on middle of distal end, and 2 long setae on middle of dorsal margin. Third podomere (2nd podomere of endopodite) of palp with 4 setae on ledge of dorso-median margin and 3 setae on anterio-distal end. Fourth (terminal) podomere bearing 2 short setae on middle of dorsal margin, 1 stout spatula-like seta with setulae along distal margin, and 3 setae on distal end.

Maxillula (Fig. 6D1, D2). Thin branchial plate (exopodite) with 25 plumose setae and 6 long reflexed setae. Basal podomere bearing 1 palp (endopodite) and 3 masticatory endites. Palp with 1 medium-length seta on middle of ventral margin, 3 medium-length setae on ledge of antero-distal margin, 1 simple and 1 spatula-like stout seta with numerous marginal setulae on distal margin. First (dorsal-most) endite bearing 2 brush-like stout seta with setulae along distal margin, and 2 short setae on antero-distal corner. Second endite with 3 short and 1 spatula-like seta on distal end. Third endite with 8 short setae on distal end and 1 short seta on middle of ventral margin.

Fifth limb (Fig. 6E) consisting of 5 articulated podomeres, length ratio among them from proximal to distal 18: 9: 6: 11: 1. First podomere with branchial plate (bearing 15 plumose setae and 2 reflexed setae on middle of ventral margin), 1 seta on anterior margin at three-fourths from proximal end, 2 setae on ledge on anterior margin at four-fifths from proximal end, and 2 long and 3 medium setae on distal end. Second podomere with 1 long and 1 medium apical seta at anterior distal corner. Third podomere with 1 medium-length apical seta at anterior distal corner. Fourth podomere with 1 short apical seta at anterior distal corner. Fifth podomere with 1 very short seta and 1 long, stout terminal claw on distal end.

Brush-shaped organ (in male) (Fig. 6H), consisting of asymmetrical paired branches. Longer and shorter branches with longer and shorter distal setae, respectively.

Sixth limb (Fig. 6F). Consisting of 5 articulated podomeres, approximate length ratio among them from proximal to distal 18: 11: 6: 13: 2. First podomere with 1 medium-length seta on anterior margin at one-third and two-thirds from proximal end, respectively, 2 medium-length setae on posterior margin at four-fifths from proximal end, and 2 short setae on distal end. Second podomere with 2 medium-length setae on antero-distal end. Third podomere with 1 medium-length apical seta at antero-distal corner. Fourth podomere with 1 short apical seta at antero-distal corner. Fifth podomere with 1 very short apical seta at antero-distal corner and 1 long terminal claw on distal end.

Seventh limb (Fig. 6G). Consisting of 5 articulated podomeres, approximate length ratio among them from proximal to distal 14: 10: 6: 15: 2. First podomere with 1 medium-length seta on anterior margin at one-third and two-thirds from proximal end, respectively, 2 medium-length setae on posterior margin at two-thirds from proximal end, 1 medium-length seta at anterior distal corner and on distal end, respectively. Second podomere with 2 apical setae at antero-distal corner. Third podomere with 1 medium-length apical seta at antero-distal corner. Fourth podomere with 1 short apical seta at antero-distal corner. Fifth podomere with 1 very short apical seta at antero-distal corner, and 1 very long terminal claw on distal end.

Furca (Fig. 7A, B) bearing 7 setae. Terminal-most 2nd seta (2) longest. Terminal-most 6th (6) and 7th (7) setae much shorter than others.

Caudal process (Fig. 7A, B). One simple seta, approximately 40–50 μm long.

Male copulatory organ (Fig. 7A). Basal capsule elliptical and consisting of some lobes. Distal lobe forming pliers-like shapes. Copulatory duct very long, curving around more than halfway of outline of basal capsule.

Female genital lobe (Fig 7B). Semicircular with doubly coiled spiral tube inside.

Dimension. See Table 1.

Occurrence. Known only from type locality.

Remarks. The carapace size of interstitial *Neonesidea* species is smaller than the epiphytic *Neonesidea* species, and the length of the adult instar of the former is approximately corresponding to the A-1 instar of the latter. The slope of the hingeline of the right valve is steep in the interstitial species, but in the epiphytic species, it is very small and almost parallel to the ventral margin. Most of the appendage morphology of *Neonesidea arenalocus* **sp. nov.** is similar to that of the other two new interstitial species, *N. alyamanai* **sp. nov.** and *N. alwakasaensis* **sp. nov.** However, *N. arenalocus* **sp. nov.** can be distinguished from the other two new species by its pliers-like distal lobe in the male copulatory organ and the twice-coiled inside tube in the female copulatory organ. A species-specific tiny spine on the posterior distal margin of the terminal claw of the male antenna is present. This new species was the interstitial *Neonesidea* sp. I examined for carapace dimensions in Ito & Tsukagoshi (2022).

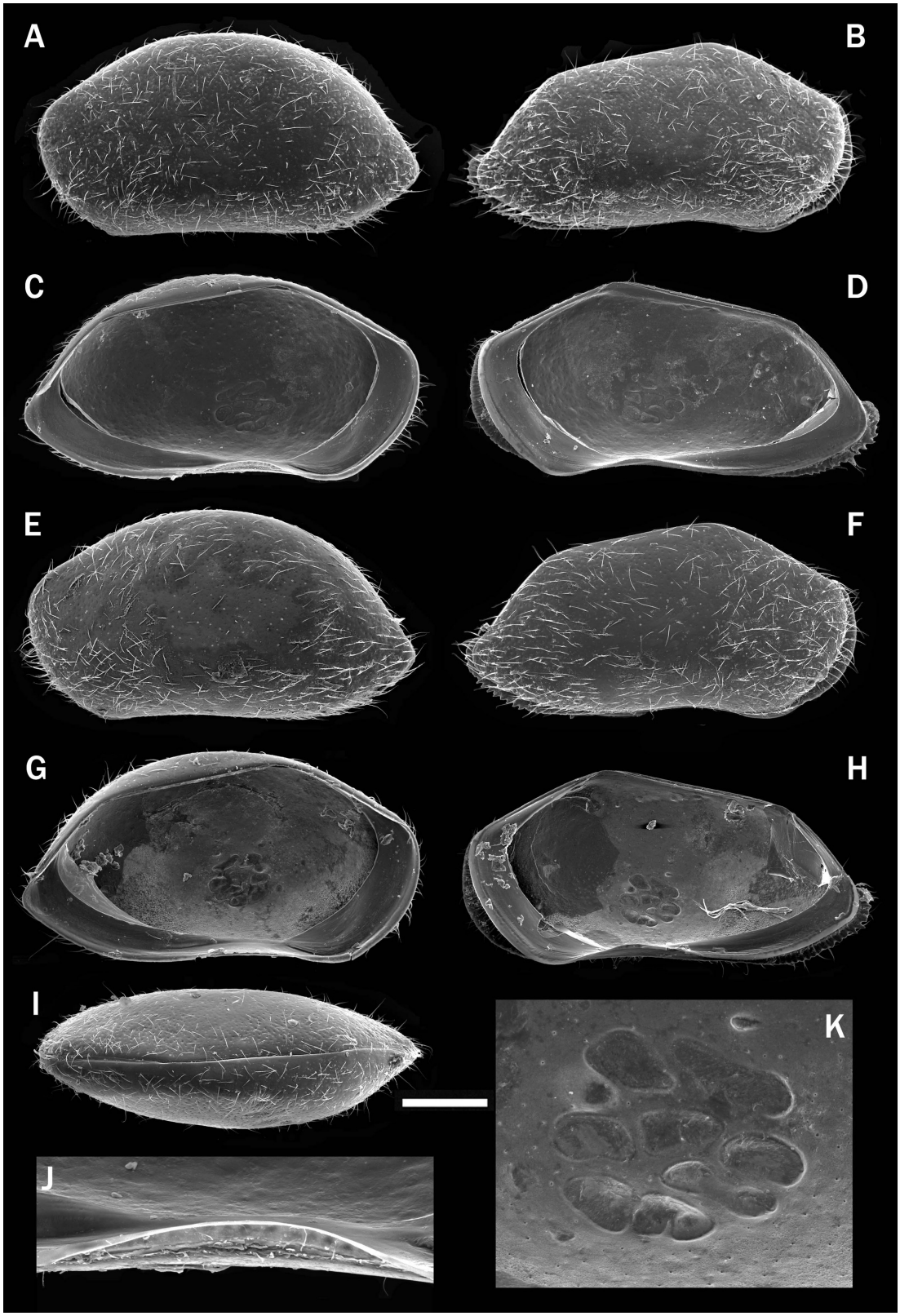

FIGURE 5. Carapace morphology of *Neonesidea arenalocus* **sp. nov.** A and B, male left and right valves, respectively (SUM-CO-2517, paratype). C and D, internal view of male left and right valves, respectively (SUM-CO-2518, paratype). E and F, external view of female left and right valves, respectively (SUM-CO-2519, paratype). G and H, internal view of female left and right valves, respectively (SUM-CO-2520, paratype). I, dorsal view of male carapace (SUM-CO-2521, paratype). J, centre of internal ventral margin of male left valve (SUM-CO-2518, paratype). K, central muscle scars on female right valve (SUM-CO-2520, paratype). Scale: 200 μm for A–I, 50 μm for J, K.

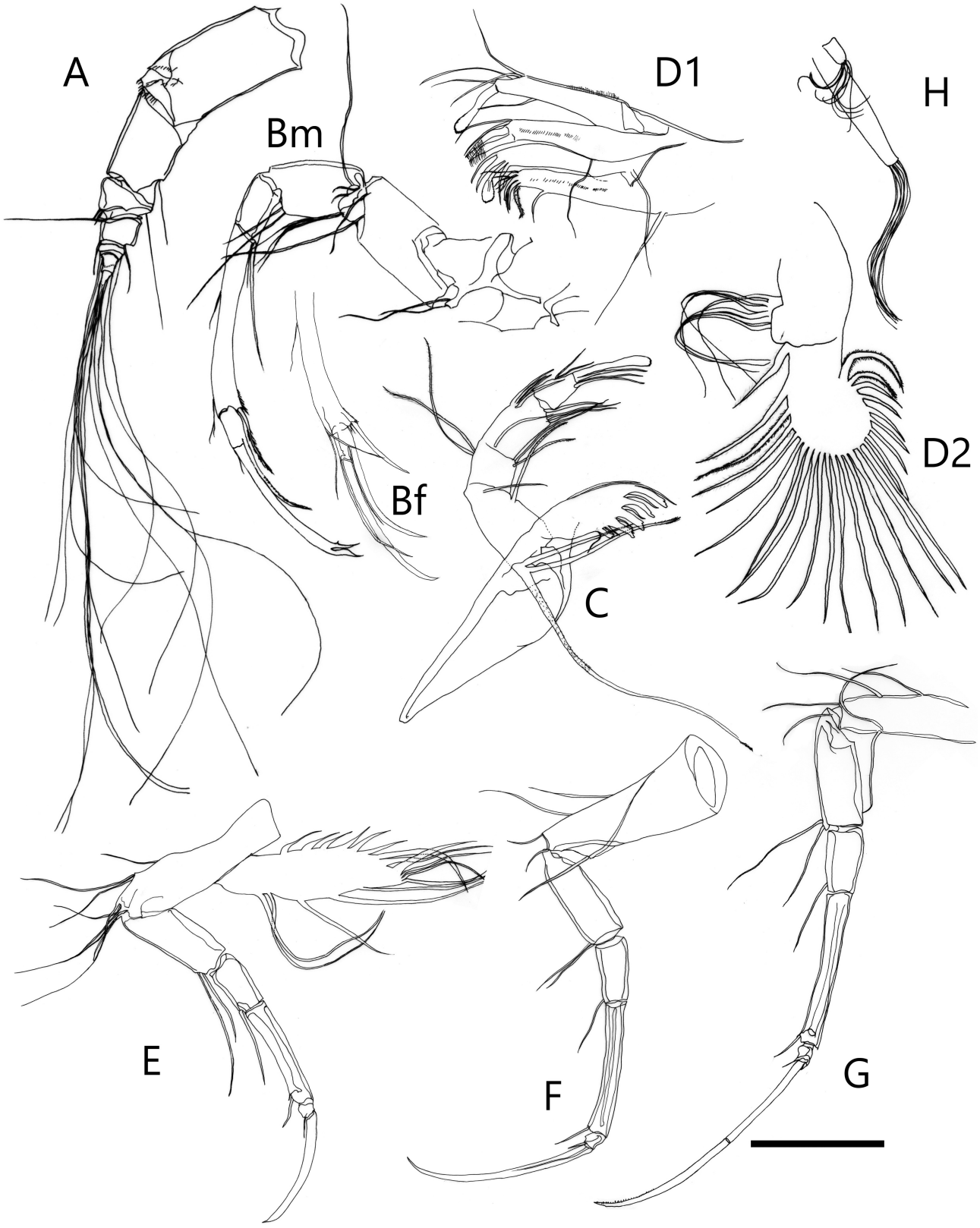

FIGURE 6. Appendages of *Neonesidea arenalocus* **sp. nov.** A, antennule; Bf, antenna of female; Bm, antenna of male, C, mandibula; D1/D2, maxillula; E, 5th limb; F, 6th limb; G, 7th limb; H, brush-shaped organ. A and C, male holotype, SUM-CO-2522; Bf, female paratype, SUM-CO-2525; Bm, H and D2, male paratype, SUM-CO-2523; D1, E, F and G, male paratype, SUM-CO-2524. Scale:100 μm.

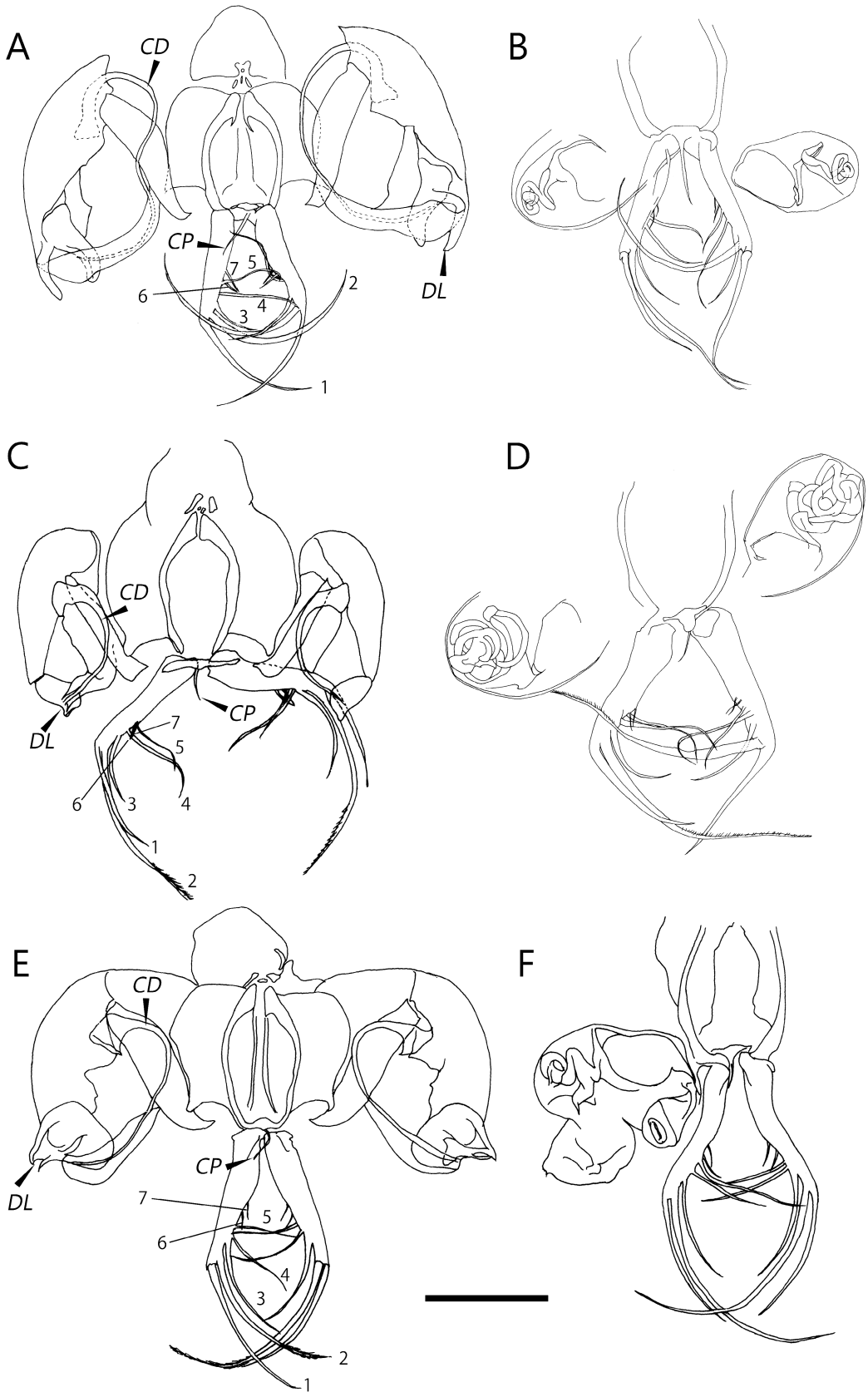

FIGURE 7. Copulatory organs, furcae, and caudal process of *Neonesidea arenalocus* **sp. nov.** (A, male holotype, SUM-CO-2522; B, female paratype, SUM-CO-2525), *Neonesidea alyamanai* **sp. nov.** (C, male holotype, SUM-CO-2532; D, female paratype, SUM-CO-2535), and *Neonesidea alwakasaensis* **sp. nov.** (E, male holotype, SUM-CO-2542; F, female paratype, SUM-CO-2544). *CD*, copulatory duct; *CP*, caudal process; *DL*, distal lobe. Setae on furcae are numbered (1–7) from distal to proximal. Scale: 100 μm.

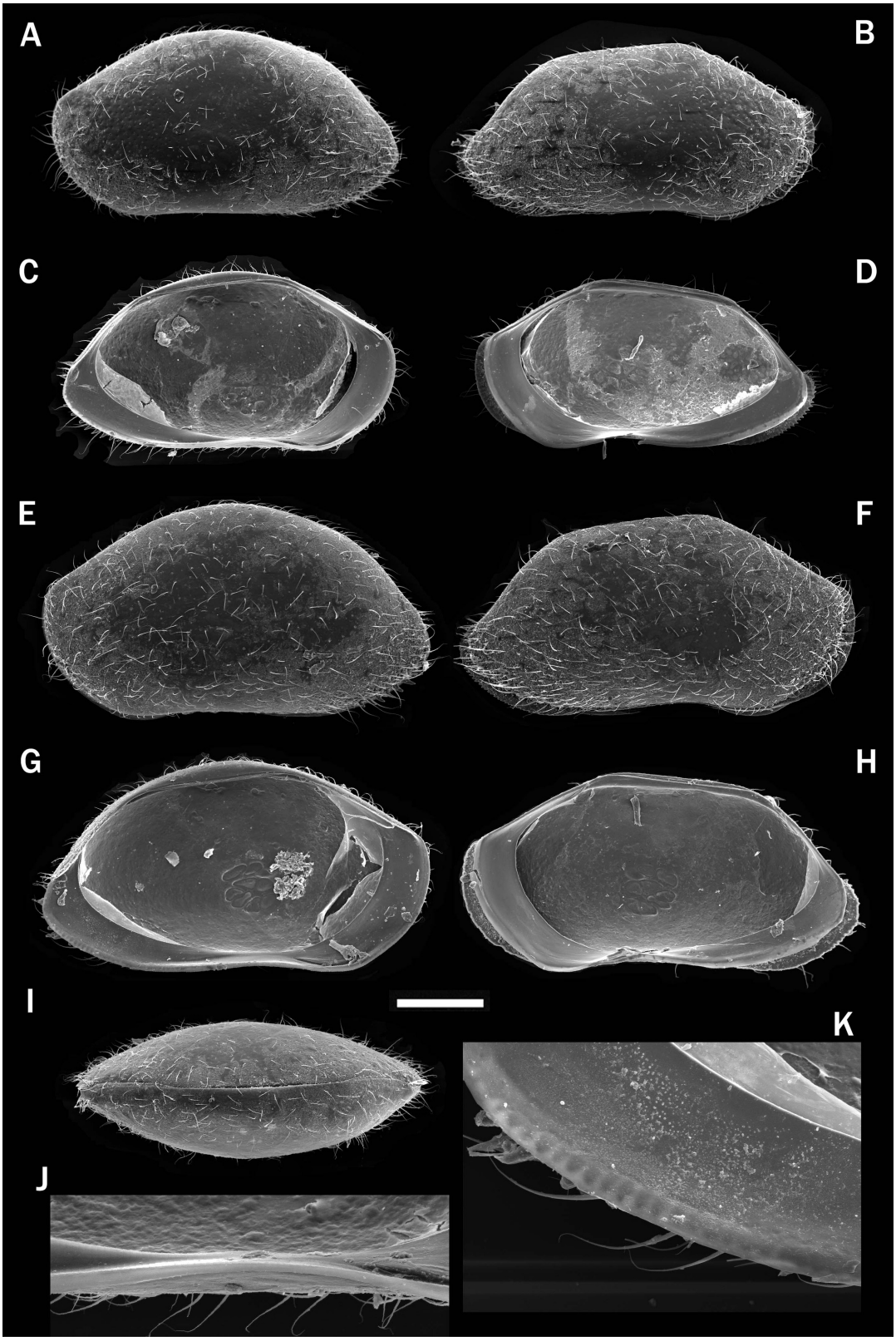

FIGURE 8. Carapace morphology of *Neonesidea alyamanai* **sp. nov.** A and B, male left and right valves, respectively (SUM-CO-2526, paratype). C and D, internal view of male left and right valves, respectively (SUM-CO-2527, paratype). E and F, external view of female left and right valves, respectively (SUM-CO-2528, paratype). G and H, internal view of female left and right valves, respectively (SUM-CO-2529, paratype). I, dorsal view of male carapace (SUM-CO-2530, paratype). J, centre of internal ventral margin of male left valve (SUM-CO-2527, paratype). K, internal posterior-ventral margin of female left valve (SUM-CO-2529, paratype). Scale: 200 μm for A–I, 50 μm for J, K.

***Neonesidea alyamanai* sp. nov.**
(Figs. 7C, D, 8, 9)

Type series. All examined specimens collected at upper infralittoral zone of coarse sand beach in Motosima Islet, Tanabe City, Wakayama Prefecture (33° 43′ 56″ N, 135° 20′ 58″ E; Loc. 2 in Fig. 1) on 19 September 2015. Holotype: adult male (SUM-CO-2532), left valve length 0.79 mm, height 0.45 mm, appendages mounted on glass slide and valves preserved in cardboard cell slide. Paratypes: 6 adult males (SUM-CO-2526, 2527, 2530, 2531, 2533 and 2534) and 3 adult females (SUM-CO-2528, 2529 and 2535).

Etymology. In honour of Dr Yusuke Yamana of Wakayama Prefectural Museum of Natural History for providing specimens of this species. Prefix "al" formed from first letters of Latin words *arena* (sand) and *locus* (space), characterising their interstitial location.

Description. *Carapace* (Fig. 8) characters almost corresponding to *Neonesidea arenalocus* **sp. nov.** Dorsal margin of right valve almost straight and nearly parallel to ventral margin. Posterior frill on right valve finely serrated. Approximately 15 auxiliary fine dentitions along interior postero-ventral margin in left valve, but no complementary structure in right valve.

Eye. Naupliar eye. No eye spot on carapace.

Antennula (Fig. 9A). Seven articulated podomeres. Chaetotaxy almost corresponding to *Neonesidea arenalocus* **sp. nov.**

Antenna (Fig. 9Bm and 9Bf). Five articulated podomeres. No tiny spine on terminal claw. Chaetotaxy almost corresponding to *Neonesidea arenalocus* **sp. nov.**

Mandible (Fig. 9C) consisting of 5 podomeres. Chaetotaxy almost corresponding to *Neonesidea arenalocus* **sp. nov.**

Maxillula (Fig. 9D1, D2). First (dorsal-most) endite bearing 2 claw-like and 2 simple short setae on distal end. Second endite with 3 short and 1 spatula-like (distal margin almost straight) setae on distal end. Other chaetotaxies almost corresponding to *Neonesidea arenalocus* **sp. nov.**

Fifth limb (Fig. 9E1, E2) consisting of 5 articulated podomeres. Chaetotaxies almost corresponding to *Neonesidea arenalocus* **sp. nov.**

Brush-shaped organ (in male) (Fig. 9H), consisting of asymmetrical paired branches. Chaetotaxy almost corresponding to *Neonesidea arenalocus* **sp. nov.**

Sixth limb (Fig. 9F). Consisting of 5 articulated podomeres. Chaetotaxy almost corresponding to *Neonesidea arenalocus* **sp. nov.**

Seventh limb (Fig. 9G). Consisting of 5 articulated podomeres. Chaetotaxy almost corresponding to *Neonesidea arenalocus* **sp. nov.**

Furca (Fig. 7C, D) bearing 7 setae. Terminal-most 2nd seta (2) nearly 2 times longer than terminal- most (1) seta. Other chaetotaxies almost corresponding to *Neonesidea arenalocus* **sp. nov.**

Caudal process (Fig. 7C, D). One simple seta, approximately 30 μm long.

Male copulatory organ (Fig. 7C). Basal capsule sub-semicircular and consisting of some lobes. Distal lobe small, short and acute. Copulatory duct arched from sub-centre of capsule to end of distal lobe.

Female genital lobe (Fig 7D). Semicircular with 3 to 4 times coiled spiral and bent tube inside.

Dimension. See Table 2.

Occurrence. Known only from type locality.

Remarks. The carapace is more similar to that of *Neonesidea arenalocus* **sp. nov.** than that of *N. alwakasaensis* **sp. nov.** because of the development of a frill in the right valve. However, the spines on the frill are finer than that in *N. arenalocus* **sp. nov.** Approximately 15 auxiliary fine dentitions along the interior posteroventral margin in the left valve were observed in this new species but not in the other two new species. The capsule of the male copulatory organ is relatively smaller than that in the other two new species, and the shape of the distal lobe is distinct. The terminal-most second seta (2) of the furca is remarkably longer than that in the other two new species.

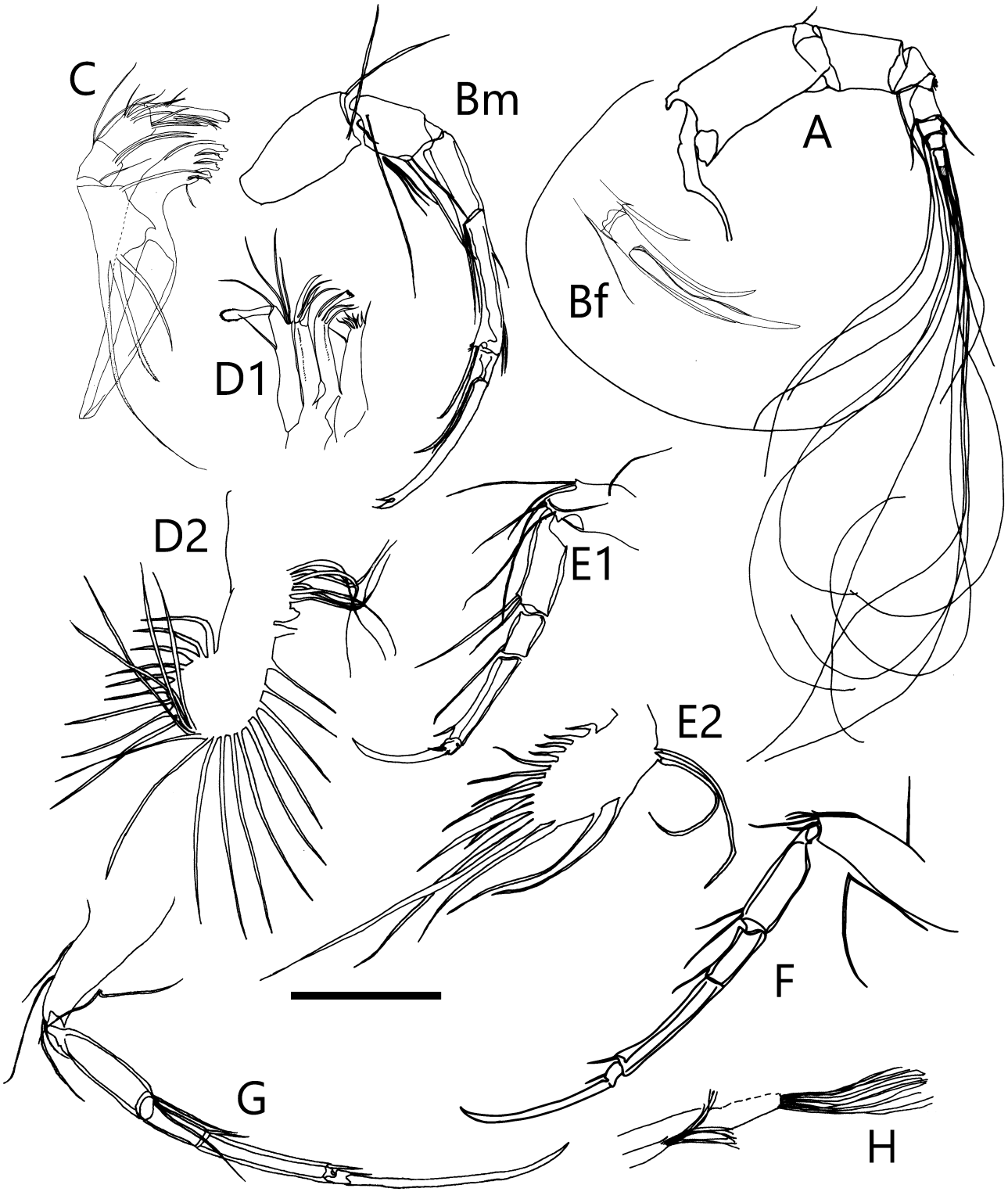

FIGURE 9. Appendages of *Neonesidea alyamanai* **sp. nov.** A, antennule; Bf, antenna of female; Bm, antenna of male; C, mandibula; D1/D2, maxillula; E1/E2, 5th limb; F, 6th limb; G, 7th limb; H, brush-shaped organ. A and Bm, male paratype, SUM-CO-2531; Bf, female paratype, SUM-CO-2535; C, D2, G and H, male holotype, SUM-CO-2532; D1, E1, E2, male paratype, SUM-CO-2533; F, male paratype, SUM-CO-2534. Scale:100 μm.

***Neonesidea alwakasaensis* sp. nov.**
(Figs. 7E, F, 10, 11)

Type series. All examined specimens collected at infralittoral zone of coarse sand beach in Tai Beach, Wakasa Bay, Kyoto Prefecture, Japan (35°34'52.8"N, 135°14'11.2"E, Loc. 3 in Fig. 1) on 9 September 2016. Holotype: adult male (SUM-CO-2542), left valve length 0.84 mm, height 0.47 mm, appendages mounted on glass slide and valves preserved in cardboard cell slide. Paratypes: 5 adult males (SUM-CO-2536, 2537, 2540, 2541, and 2543) and 3 adult females (SUM-CO-2538, 2539 and 2544).

Etymology. After name of type locality, Wakasa Bay. Prefix "al" formed from first letters of Latin words *arena* (sand) and *locus* (space), characterising their interstitial habitat.

Description. *Carapace* (Fig. 10) characters almost corresponding to *Neonesidea arenalocus* **sp. nov.** Dorsal margin of valve weakly arched and making waterdrop-like outline. Approximately 12 small but conspicuous spines along postero-ventral margin of right valve. Frills along anterior and posterior margins not developed. No auxiliary dentitions along interior margin.

Eye. Naupliar eye. No eye spot on carapace.

Antennula (Fig. 11A). Seven articulated podomeres. Chaetotaxy almost corresponding to *Neonesidea arenalocus* **sp. nov.**

Antenna (Fig. 11Bm and 11Bf). Five articulated podomeres. Chaetotaxy almost corresponding to *Neonesidea arenalocus* **sp. nov.**

Mandible (Fig. 11C) consisting of 5 podomeres. Chaetotaxy almost corresponding to *Neonesidea arenalocus* **sp. nov.**

Maxillula (Fig. 11D1, D2). Chaetotaxies almost corresponding to *Neonesidea alyamanai* **sp. nov**.

Fifth limb (Fig. 11E1, E2) consisting of 5 articulated podomeres. Chaetotaxies almost corresponding to *Neonesidea arenalocus* **sp. nov.**

Brush-shaped organ (in male) (Fig. 11H), consisting of extremely asymmetrical paired branches. Well-developed branch with more than 10 setae on distal end and 6 conspicuous annulations. Smaller brunch with several setae.

Sixth limb (Fig. 11F). Consisting of 5 articulated podomeres. Chaetotaxy almost corresponding to *Neonesidea arenalocus* **sp. nov.**

Seventh limb (Fig. 11G). Consisting of 5 articulated podomeres. Chaetotaxy almost corresponding to *Neonesidea arenalocus* **sp. nov.**

Furca (Fig. 7E, F) bearing 7 setae. Terminal-most 2nd seta (2) almost same length as terminal-most (1) seta. Other chaetotaxies almost corresponding to *Neonesidea arenalocus* **sp. nov.**

Caudal process (Fig. 7E, F). One simple short seta, approximately 20 μm long.

Male copulatory organ (Fig. 7E). Basal capsule sub-semicircular and consisting of some lobes. Distal lobe shaped like the head of Raptores. Copulatory duct bending largely at proximal part.

Female genital lobe (Fig 7F). Semicircular main lobe with coiled spiral and bent tube inside. Two derivative lobes at proximal end and middle of main lobe.

Dimension. See Table 3.

Occurrence. Known only from type locality.

Remarks. The general shape of the carapace is similar to that of the other two species, *Neonesidea arenalocus* **sp. nov.** and *N. alyamanaensis* **sp. nov.** However, this new species does not have a frill in the right valve or auxiliary dentitions along the interior margin. Instead, this new species has approximately 12 small but conspicuous spines along the postero-ventral margin of the right valve. The shape of the distal lobe of the male copulatory organ in this new species is distinguishable from the other two new species. The terminal-most (1) and second-most terminal (2) setae of the furca were almost the same length. The brush-shaped organ in this new species is also distinguishable from that in the other two new species because of the extremely asymmetrical paired branches and the well-developed branch with six conspicuous annulations.

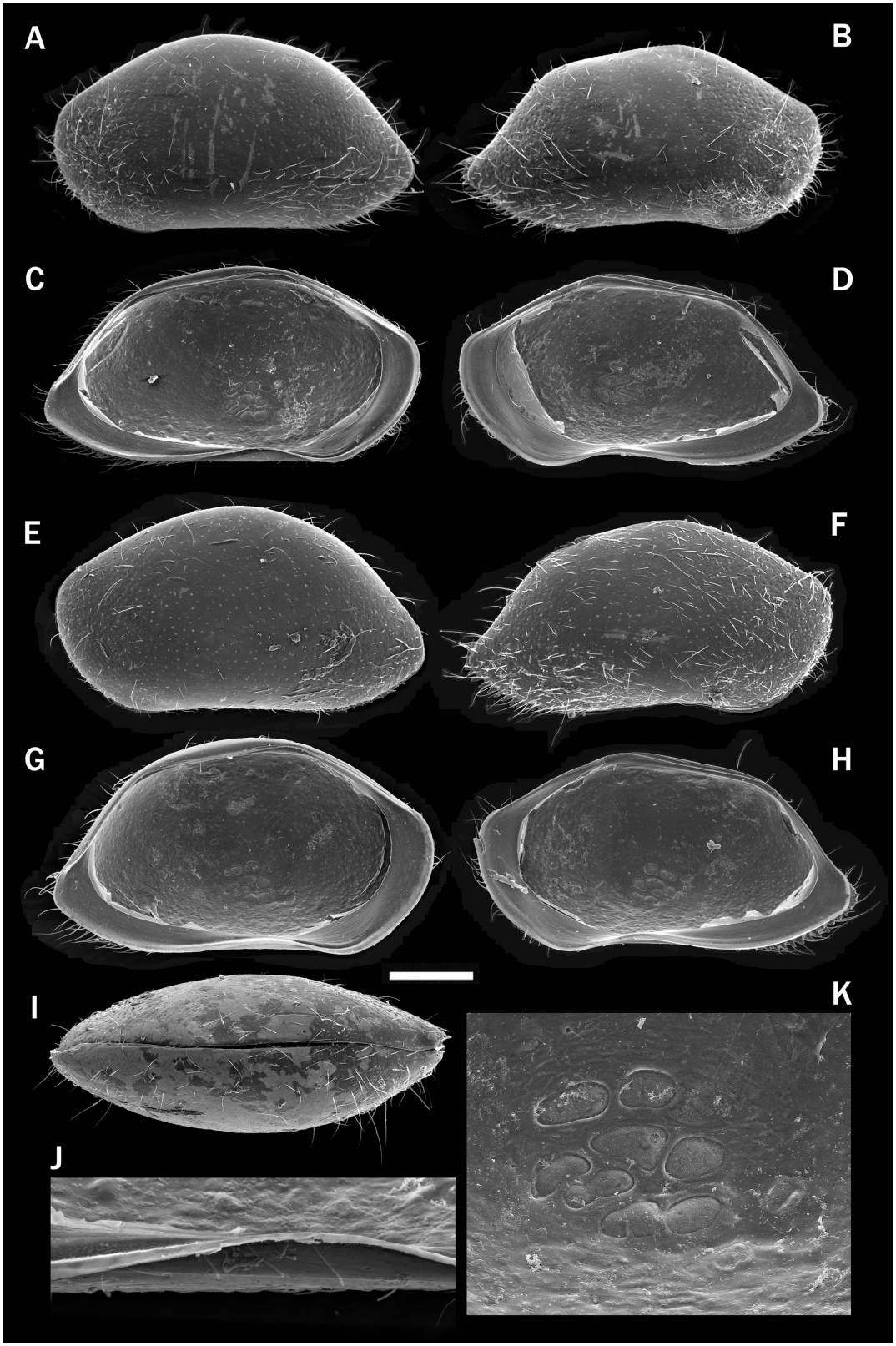

FIGURE 10. Carapace morphology of *Neonesidea alwakasaensis* **sp. nov.** A and B, male left and right valves, respectively (SUM-CO-2536, paratype). C and D, internal view of male left and right valves, respectively (SUM-CO-2537, paratype). E and F, external view of female left and right valves, respectively (SUM-CO-2538, paratype). G and H, internal view of female left and right valves, respectively (SUM-CO-2539, paratype). I, dorsal view of male carapace (SUM-CO-2540, paratype). J, centre of internal ventral margin of male left valve (SUM-CO-2537, paratype). K, central muscle scars on female left valve (SUM-CO-2539, paratype). Scale: 200 μm for A–I, 50 μm for J, K.

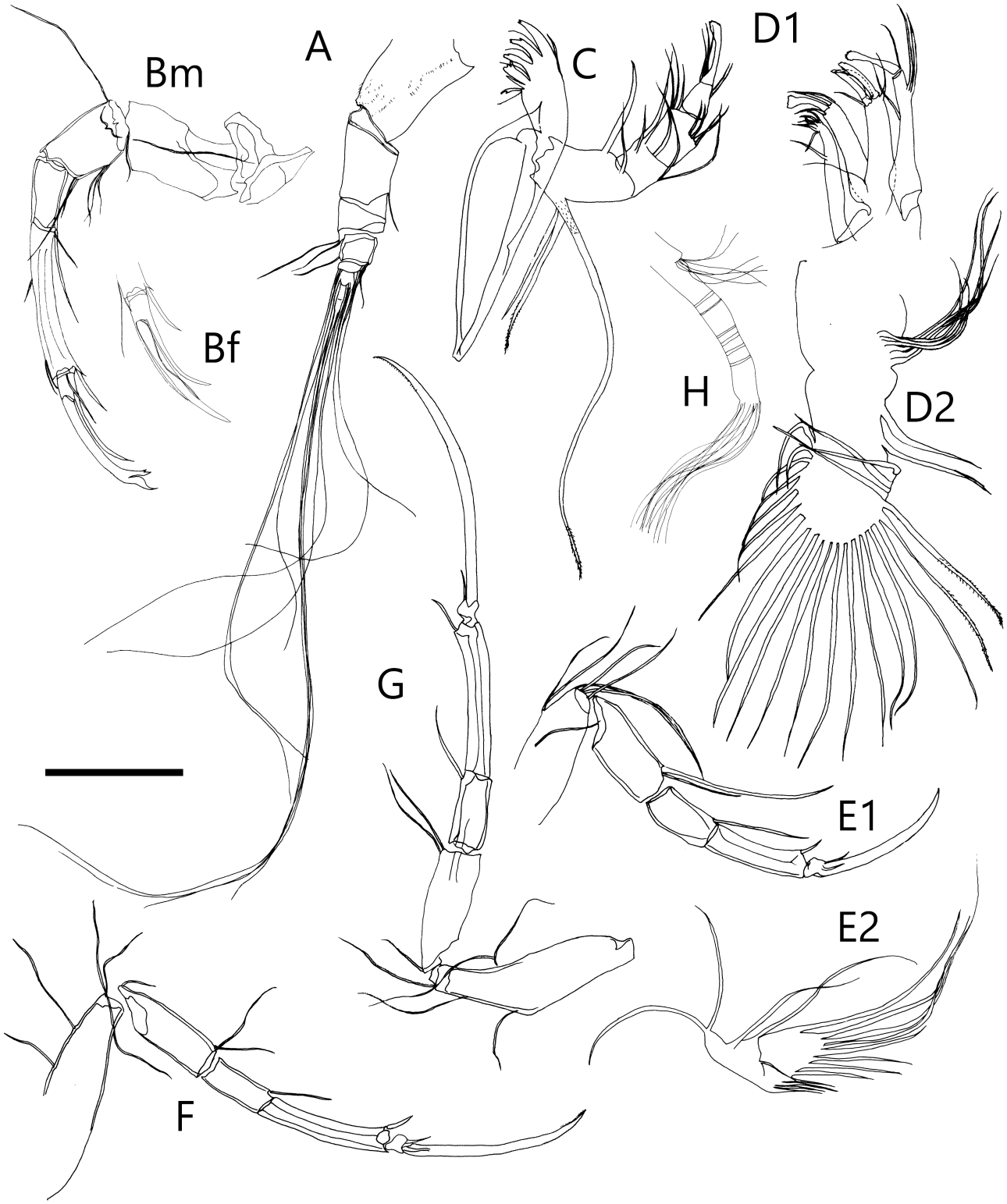

FIGURE 11. Appendages of *Neonesidea alwakasaensis* **sp. nov.** A, antennule; Bf, antenna of female; Bm, antenna of male; C, mandibula; D1/D2, maxillula; E1/E2, 5th limb; F, 6th limb; G, 7th limb; H, brush-shaped organ. A and D2, male paratype, SUM-CO-2541; Bf, female paratype, SUM-CO-2544; Bm, C, E1, E2, F and G, male holotype, SUM-CO-2542; D1 and H, male paratype, SUM-CO-2543. Scale:100 μm.

TABLE 1. Dimension of valves of *Neonesidea arenalocus* **sp. nov.**

		Length		Height		Width		
		AV	OR	AV	OR	AV	OR	*N*
Male	RV	0.89	0.85 – 0.91	0.42	0.40 – 0.44	0.17	0.13 – 0.19	7
	LV	0.87	0.83 – 0.89	0.45	0.44 – 0.45	0.17	0.16 – 0.20	5
Female	RV	0.89	0.86 – 0.92	0.41	0.37 – 0.43	0.17	0.13 – 0.22	7
	LV	0.90	0.87 – 0.93	0.49	0.45 – 0.51	0.21	0.19 – 0.22	5

TABLE 2. Dimension of valves of *Neonesidea alyamanai* **sp. nov.**

		Length		Height		Width		
		AV	OR	AV	OR	AV	OR	*N*
Male	RV	0.81	0.80 – 0.83	0.40	0.40 – 0.41	0.16	0.14 – 0.19	5
	LV	0.79	0.75 – 0.82	0.45	0.42 – 0.49	0.17	0.15 – 0.19	6
Female	RV	0.91	0.90 – 0.91	0.48	0.47 – 0.48	0.16	0.14 – 0.18	2
	LV	0.89	0.89 – 0.89	0.50	0.50	0.19	0.19	2

TABLE 3. Dimension of valves of *Neonesidea alwakasaensis* **sp. nov.**

		Length		Height		Width		
		AV	OR	AV	OR	AV	OR	*N*
Male	RV	0.85	0.82 – 0.89	0.42	0.40 – 0.44	0.18	0.17 – 0.21	5
	LV	0.87	0.84 – 0.90	0.45	0.44 – 0.46	0.19	0.17 – 0.20	4
Female	RV	0.87	0.84 – 0.91	0.44	0.42 – 0.47	0.18	0.18 – 0.20	6
	LV	0.87	0.84 – 0.90	0.50	0.48 – 0.52	0.21	0.20 – 0.22	6

Discussion

Many species of the genus *Neonesidea* have been described, but this is the first report of interstitial species of this genus. To date, the interstitial species of the superfamily Bairdioidea are known only from the family Pussellidae. The interstitial pusselliid species exhibit characteristics distinctly different in each genus, for example, *Pussella*, *Danipussella*, *Anchistrocheles*, and so on. However, the three new interstitial species of *Neonesidea* do not exhibit essential differences from the epiphytic *Neonesidea* species, except for the small width of the carapace and linear claw of the walking legs, which are considered adaptations for the interstitial environment. Indeed, characteristics of chitinous parts that determine this genus, like the bifurcated tip of the male antenna and the chaetotaxy of furca, are preserved. Whether these three interstitial species are monophyletic with respect to other epiphytic *Neonesidea* species cannot be addressed at this time. Molecular phylogenetic analyses are needed for further elucidation.

Watanabe *et al.* (2008) showed that optimal zones based on distance from the strand line are formed in the intertidal zone in interstitial ostracods. In this study, the optimal zone for *Neonesidea arenalocus* **sp. nov.** is shown in the upper infralittoral zone (Fig. 2). The grain-size composition among the eight collecting points did not differ significantly (Fig. 3); therefore, other factors like the susceptibility of sediments to be moved by waves could be an influence. Since the influence is strong around the strand line, sediments become unstable; meanwhile, the oxygen level decreases at points far from the strand line. The three new interstitial species retain their naupliar eyes. They probably inhabit parts relatively close to the surface of the sediment. Their naupliar eyes are probably used to detect the possibility of being washed out on the sediment surface. Watanabe *et al.* (2008) found that interstitial *Microloxoconcha ikeyai* Watanabe *et al.,* 2008 with eyes have a negative phototaxis to light. Phototaxis was not tested for *N. arenalocus* **sp. nov.**, but we observed that it is rarely found in the surface sediments at each point.

The sampling site Loc. 1 (Figs. 1 and 2) provided information on ostracods, including undescribed taxa in the upper infralittoral zone. Namely, *Parapolycope* spp., *Parvocythere japonica* Watanabe *et al.,* 2008, *Parvocythere* spp., and *Cobanocythere* sp. can also be found in the intertidal zone at the same beach. In contrast, *Semicytherura sagittiformis* Yamada & Tanaka, 2011, undescribed *Cytherois* sp., and *Tribelina* sp. are found in the upper infralitto-

ral zone rather than the intertidal zone. Apart from the genus *Neonesidea*, this is the first report of interstitial species of the genera *Cytherois* and *Tribelina*. These suggest that adaptation to the interstitial environment in the infralittoral zone is a preliminary step to adaptation to the harsh environmental conditions of the intertidal zone, which includes phases of drying out and freshwater inflow.

The small carapace width of the interstitial ostracods was reported by Ito & Tsukagoshi (2022), with a characteristic change through ontogeny. In contrast, the X-ray micro-CT scan images provided a few novel aspects between the epiphytic and interstitial *Neonesidea* species (Fig. 12). The interstitial species not only have small carapace widths, but also extremely thin carapaces, approximately less than one-fourth the thickness of those of the epiphytic species. Moreover, the position of the maximum carapace width is approximately at the centre for the epiphytic species, whereas it is at the lower (ventral) end for the interstitial species. This is similar to the difference between the phytal and sand-bottom species of the genus *Loxoconcha* (Kamiya 1988). Two extreme trends can be found in the carapace morphology of interstitial podocopan ostracods. One type has a small carapace width like *Microloxoconca* species and *Anchistrocheles* species, and the other has a subtriangular cross-section with a well-developed ventral ridge like *Semicytherura sagittiformis* and *Cobanocythere* species. The former is probably an adaptation for crawling through the gaps between sediment particles, and the latter is probably an adaptation for stable grounding on the sediment grain surface. The interstitial *Neonesidea* species can be said to be an intermediate state between the two. As interstitial species, the three *Neonesidea* species shown here have a relatively large carapace. Probably the degree of morphological differentiation from the common ancestor, thought to have lived on seaweeds, is not very large. Their morphology is thought to be adapted to the interstitial environment while retaining the traits of their common ancestor.

TABLE 4. Dimension of A and B values for curvature evaluation of terminal claws of 5th to 7th limbs in interstitial and epiphytic *Neonesidea* species.

<Interstitial species>

A *Neonesidea arenalocus* sp. nov.

Specimen No. /Limb	5th limb	6th limb	7th limb
1	0.15	0.15	0.15
2	0.15	0.14	0.15
3	0.18	0.13	0.12
4	0.19	0.13	0.15
5	0.14	0.12	0.14
6	0.20	0.14	0.15
7	0.13	0.11	0.13
8	0.19	0.13	0.12
Av.	0.17	0.13	0.14

B *Neonesidea alyamanai* sp. nov.

Specimen No. /Limb	5th limb	6th limb	7th limb
1	0.20	0.15	0.15
2	0.19	0.14	0.12
3	0.20	0.13	0.11
4	0.17	0.13	0.13
5	0.22	0.17	0.13
6	0.19	0.16	0.14
7	0.20	0.16	0.14
8	0.20	0.16	0.14
Av.	0.20	0.15	0.13

C *Neonesidea alwakasaensis* sp. nov.

Specimen No. /Limb	5th limb	6th limb	7th limb
1	0.16	0.15	0.17
2	0.20	0.15	0.14
3	0.18	0.15	0.14
4	0.18	0.16	0.15
5	0.17	0.16	0.16
6	0.20	0.14	0.16
7	0.15	0.14	0.14
8	0.16	0.14	0.14
Av.	0.18	0.15	0.15

<Epiphytic species>

D *Neonesidea* sp. 1

Specimen No. /Limb	5th limb	6th limb	7th limb
1	0.25	0.23	0.20
2	0.22	0.20	0.20
3	0.23	0.24	0.21
4	0.23	0.23	0.22
5	0.26	0.20	0.23
6	0.24	0.24	0.24
7	0.23	0.21	0.23
Av.	0.24	0.22	0.22

E *Neonesidea* sp. 2

Specimen No. /Limb	5th limb	6th limb	7th limb
1	0.23	0.22	0.18
2	0.22	0.17	0.18
Av.	0.23	0.19	0.18

F *Neonesidea* sp. 3

Specimen No. /Limb	5th limb	6th limb	7th limb
1	0.22	0.26	0.23
2	0.24	0.25	0.24
Av.	0.23	0.25	0.24

G Comparison of averages between interstitial and epiphytic speceies

Habitat/Limb	5th limb	6th limb	7th limb
3 interstitial species	0.18	0.14	0.14
3 epiphytic species	0.23	0.22	0.21

Adaptation to the interstitial environment can be considered along with the differences in the curvature of the terminal claw. The fifth, sixth, and seventh limbs of the *Neonesidea* species are recognised as walking legs in functional view. This study indicated large differences in the curvature of the claw on the terminal of the legs, between the interstitial and epiphytic species (Fig. 4 and Table 4). This difference is considered to be dependent on the behaviour of both the interstitial and epiphytic species. Kamiya (1988) reported the difference in the shape of the terminal claw between the phytal species *Loxoconcha japonica* Ishizaki, 1968 and the sand-bottom species *Loxoconcha uranouchiensis* Ishizaki, 1968. He explained that the former developed a hook-like shape on the tip of the claw to hold their body on the leaves of seagrasses, which are shaken by waves. The epiphytic *Neonesidea* species have high-curvature terminal claws. This high curvature is considered necessary to inhabit seaweeds growing on the bedrock. In contrast, it is considered that the interstitial *Neonesidea* species have near-straight terminal claws to inhabit narrow spaces by ensuring stability on sediments and crawling between sand grains.

Horikoshi *et al.* (2019) underscored the possibility that the asymmetrical brush-shaped organ in *Neonesidea* and closely related genera is a synapomorphic characteristic of the family Bairdiidae. We observed the asymmetrical brush-shaped organ in all three new species, enhancing the possibility of it being a synapomorphic characteristic. The taxonomic potential of the furca was also observed. These three new species and *Neonesidea ikayai* Horikoshi *et al.,* 2019 share a certain chaetotaxy with minor specific differences.

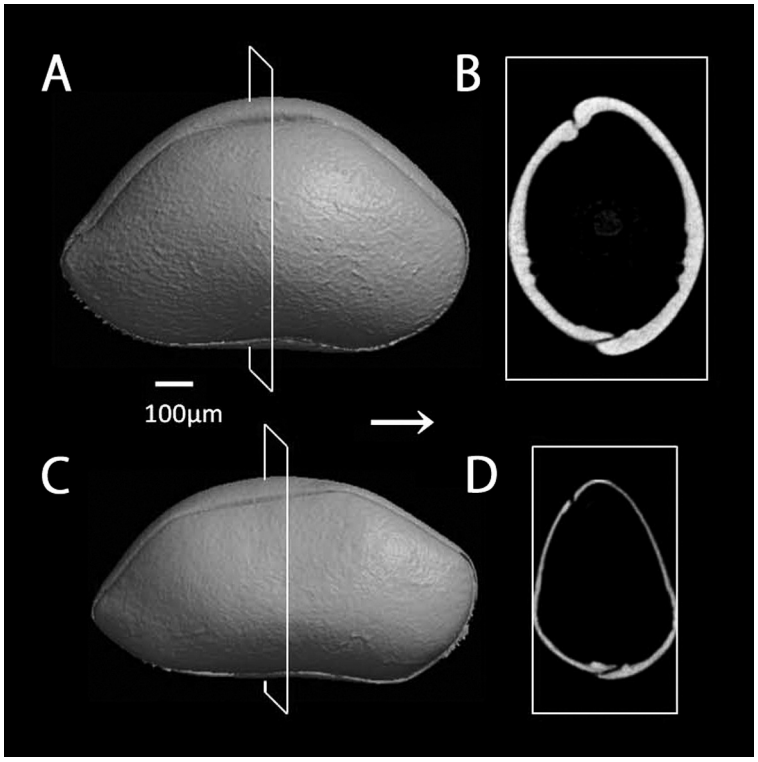

FIGURE 12. Carapace images by the X-ray micro CT scan in epiphytic *Neonesidea* sp. (A, B) and interstitial *N. arenalocus* **sp. nov.** (C, D). A and C, right lateral views; B and D, transversal views from anterior.

Acknowledgements

The authors appreciate Dr Hayato Tanaka (Tokyo Sea Life Park, Tokyo, Japan) and Dr Yusuke Yamana (Wakayama Prefectural Museum of Natural History, Wakayama, Japan) for their valuable suggestions and the specimens from Tanabe Bay; Dr Osamu Sasaki (Tohoku University, Sendai, Japan) and Dr Ryouichi Higashi (Shizuoka Prefectural Arai High School, Kosai City, Japan) for their support by taking photos by the X-ray mirco-CT scan; Mr Hideyuki Horikoshi, Mr Daigo Miyata, Ms Misumi Ito, and Mr Keisuke Hosaka (Shizuoka University, Shizuoka, Japan), and the members of the Ostracod Research Team of Shizuoka University for their continuous encouragement.

This study was partially supported by the Aids for Scientific Research [grant numbers 16K07478, 20H03309] from the Japanese Society for the Promotion of Science.

References

Brandão, S.N. (2022) World Register of Marine Species –*Neonesidea* Maddocks, 1969. Available from: https://www.marinespecies.org/aphia.php?p=taxdetails&id=127568 (accessed 30 September 2022)

Cerca, J., Purschke, G. & Struck, T.H. (2018) Marine connectivity dynamics: clarifying cosmopolitan distributions of marine interstitial invertebrates and the meiofauna paradox. *Marine Biology*, 165, 123. https://doi.org/10.1007/s00227-018-3383-2

Ha, T.M. & Tsukagoshi, A. (2015) First records of interstitial leptocytherids (Crustacea, Ostracoda): two new species and a redescription of *Callistocythere ventricostata* Ruan & Hao, 1988 collected from the Okinawa Islands, southern Japan. *Zootaxa*, 4006 (1), 83–102. https://doi.org/10.11646/zootaxa.4006.1.4

Higashi, R. & Tsukagoshi, A. (2008) Two new species of *Microloxoconcha* (Crustacea: Ostracoda: Podocopida) from Japan, with redescription of the genus. *Species Diversity*, 13, 157–173. https://doi.org/10.12782/specdiv.13.157

Higashi, R. & Tsukagoshi, A. (2011) Four new species of the interstitial family Cobanocytheridae (Crustacea: Ostracoda) from central Japan. *Zootaxa*, 2924 (1), 33–56. https://doi.org/10.11646/zootaxa.2924.1.3

Higashi, R. & Tsukagoshi, A. (2012) Two new species of the interstitial genus *Parvocythere* (Crustacea, Ostracoda, Cytheroidea) from Japan: an example of morphological variation. *ZooKeys*, 193, 27–48. https://doi.org/10.3897/zookeys.193.2842

Higashi, R., Tsukagoshi, A., Kimura, H. & Kato, K. (2011) Male dimorphism in a new interstitial species of the genus *Microloxoconcha* (Podocopida: Ostracoda). *Journal of Crustacean Biology*, 31, 142–152. https://doi.org/10.1651/09-3234.1

Hiruta, S. (1983) A new species of the genus *Polycope* Sars from the Inland Sea of Japan (Ostracoda: Cladocopina). *Proceedings of the Japanese Society of Systematic Zoology*, 26, 1–10.

Hiruta, S. (1989) A new species of marine interstitial Ostracoda of the genus *Microloxoconcha* Hartmann from Hokkaido, Japan. *Proceedings of the Japanese Society of Systematic Zoology*, 39, 29–36.

Hiruta, S. (1991) A new species of marine interstitial Ostracoda of the genus *Psammocythere* Klie from Hokkaido, Japan. *Zoological Science*, 8, 113–120.

Hiruta, S.F., Hiruta, S. & Mawatari, S.F. (2007) A new, interstitial species of *Terrestricythere* (Crustacea: Ostracoda) and its microdistribution at Orito Beach, northeastern Sea of Japan. *Hydrobiologia*, 585, 43–56. https://doi.org/10.1007/s10750-007-0627-4

Horikoshi, H. Nakao, Y. & Tsukagoshi, A. (2019) Two new species of Bairdiidae (Ostracoda: Crustacea) from the western Pacific coast of Japan. *Zootaxa*, 4679 (3), 450–462. https://doi.org/10.11646/zootaxa.4679.3.2

Horne, D.J., Cohen, A. & Martens, K. (2002) Taxonomy, morphology and biology of Quaternary and living Ostracoda. *In:* Holmes, J.A. & Chivas, A.R. (Eds.), *The Ostracoda—Applications in Quaternary Research.* Washington, DC, *American Geophysical Union Geophysical Monograph*, 131, 5–36. https://doi.org/10.1029/131GM02

Howe, H.V. (1955) Handbook of Ostracod Taxonomy. *Louisiana State University Studies*, *Physical Science Series*, 1, 1–386. https://doi.org/10.5962/bhl.title.10240

Ishizaki, K. (1968) Ostracodes from Uranouchi Bay, Kochi Prefecture, Japan. *Science Reports of the Tohoku University, Sendai, Japan*, Series 2 (Geology), 40, 1–45.

Ito, M. & Tsukagoshi, A. (2022) Two species of the genus *Anchistrocheles* (Bairdioidea: Ostracoda: Crustacea) from Japan and their developmental characteristics for adaptation to interstitial environments. *Zootaxa*, 5194 (1), 71–91. https://doi.org/10.11646/zootaxa.5194.1.4

Kamiya, T. (1988) Morphological and ethological adaptations of Ostracoda to microhabitats in *Zostera* beds. *In*: Hanai, T., Ikeya, N. & Ishizaki, K. (Eds.), *Evolutionary Biology of Ostracoda: its Fundamentals and Applications*. Kodansha-Elsevier, Tokyo, pp. 303–318. https://doi.org/10.1016/S0920-5446(08)70191-2

Maddocks, R.F. (1969) Revision of Recent Bairdiidae (Ostracoda). *United States National Museum Bulletin*, 295, 1–126. https://doi.org/10.5479/si.03629236.295.1

Sars, G.O. (1888) Nye bidrag til kundskaben om Middelhavets invertebratfauna. IV, Ostracoda mediterranea (sydeuropæiske Ostracoder). *Archiv for mathematik og naturvidenskab*, 12, 173–324. https://doi.org/10.5962/bhl.title.10252

Tanaka, H. (2013) The mating behaviour of the seed shrimp *Parapolycope spiralis* (Ostracoda: Cladocopina), with insight into the evolution of mating systems in cryptic interstitial habitats. *Biological Journal of the Linnean Society*, 109, 791–801. https://doi.org/10.1111/bij.12080

Tanaka, H., Kondo, Y. & Ohtsuka, S. (2020) *Pontopolycope orientalis* sp. nov. (Crustacea: Ostracoda: Polycopidae), the first report of a living species of the genus from the Indo-Pacific region. *Zoological Studies*, 59, 1–12.

Tanaka, H. & Ohtsuka, S. (2016) Historical biogeography of the genus *Polycopissa* (Ostracoda: Myodocopa: Cladocopina),

with the description and DNA barcode of the second Indo-Pacific species from the Seto Inland Sea. *Marine Biodiversity*, 46, 625–640.
https://doi.org/10.1007/s12526-015-0412-y
Tanaka, H. & Ohtsuka, S. (2019) Two new species of *Microloxoconcha* (Crustacea: Ostracoda) from the sublittoral zone in western Japan. *Species Diversity*, 24, 217–228.
https://doi.org/10.12782/specdiv.24.217
Tanaka, H. & Tsukagoshi, A. (2010) Two new interstitial species of the genus *Parapolycope* (Crustacea: Ostracoda) from central Japan. *Zootaxa*, 2500 (1), 39–57.
https://doi.org/10.11646/zootaxa.2500.1.2
Tanaka, H. & Tsukagoshi, A. (2013a) Description and scanning electron microscopic observation of a new species of the genus *Polycopetta* (Crustacea, Ostracoda, Cladocopina) from an interstitial habitat in Japan. *ZooKeys*, 294, 75–91.
https://doi.org/10.3897/zookeys.294.4846
Tanaka, H. & Tsukagoshi, A. (2013b) The taxonomic utility of the male upper lip morphology in the ostracod genus *Parapolycope* (Crustacea), with descriptions of two new species. *Journal of Natural History*, 47, 963–986.
https://doi.org/10.1080/00222933.2012.743615
Tanaka, H. & Tsukagoshi, A. (2014) Intraspecific variation in male upper lip morphology of *Parapolycope watanabei* n. sp. (Crustacea: Ostracoda) and its implications for speciation. *Zoological Science*, 31, 758–765.
https://doi.org/10.2108/zs140128
Tanaka, H., Tsukagoshi, A. & Hiruta, S. (2010) A new combination in the genus *Parapolycope* (Crustacea: Ostracoda: Myodocopa: Cladocopina), with the description of a new species from Japan. *Species Diversity*, 15, 93–108.
https://doi.org/10.12782/specdiv.15.93
Tanaka, H., Tsukagoshi, A. & Karanovic, I. (2014) Molecular phylogeny of interstitial Polycopidae ostracods (Crustacea) and descriptions of a new genus and four new species. *Zoological Journal of the Linnean Society*, 172, 282–317.
https://doi.org/10.1111/zoj.12176
Tsukagoshi, A. (2017) Studies on the living organisms for paleontology, part 2: Case studies for evolution and biodiversity of ostracods. *Fossils*, 102, 15–30. [in Japanese]
Van Morkhoven, F.P.C.M. (1963) *Post-Paleozoic Ostracoda, their morphology, taxonomy, and economic use, Volume 2 Generic descriptions*. Elsevier, Amsterdam, 478 pp.
Watanabe, S., Tsukagoshi, A. & Higashi, R. (2008) Taxonomy and ecology of two new interstitial cytheroid Ostracoda (Crustacea) from Shimoda, central Japan. *Species Diversity*, 13, 53–71.
https://doi.org/10.12782/specdiv.13.53
Yamada, S. & Tanaka, H. (2011) First report of an interstitial *Semicytherura* (Crustacea: Ostracoda: Cytheruridae: Cytherurinae): a new species from central Japan. *Species Diversity*, 16, 49–63.
https://doi.org/10.12782/specdiv.16.49
Yamada, S. & Tanaka, H. (2013) Two interstitial species of the genus *Semicytherura* (Crustacea: Ostracoda) from Japan, with notes on their microhabitats. *Zootaxa*, 3745 (4), 435–448.
https://doi.org/10.11646/zootaxa.3745.4.2